

RESEARCH

Open Access



Dexamethasone-induced whitening of rabbit brown adipose tissue: leptin resistance and mitochondrial dysfunction

Xiaoqin Tang¹, Beibei Zhang², Puhang Xie², Yanpei Wei¹, Yanbo Qiu¹, Xiaohua Yi¹, Ziru Zhang², Muzi She², Xiuzhu Sun^{2*} and Shuhui Wang^{1*}

Abstract

Background Research on the effects of exogenous glucocorticoids on brown adipose tissue (BAT) is crucial for understanding how these hormones can induce metabolic disorders such as obesity. In this study, we explored the effects of glucocorticoids, specifically dexamethasone (Dex), on the metabolic transformation of BAT to white adipose tissue (WAT).

Results Our results indicate a significant whitening shift in BAT upon Dex treatment, characterized by increased lipid deposition, decreased mitochondrial density, a significant decline in cellular ATP content, and reduced expression of mitochondrial markers. We demonstrate the crucial role of leptin resistance in mediating mitochondrial function through the overexpression and inhibition of *LEPR*.

Conclusions Our results suggest the role of leptin resistance in regulating of mitochondrial biogenesis and energy metabolism in glucocorticoid-induced brown adipose whiteness.

Keywords Dexamethasone, Brown adipose tissue whitening, Mitochondrial dysfunction

Background

Brown adipose tissue (BAT) specializes in energy expenditure and heat production, while white adipose tissue (WAT) stores energy. Both are important for metabolism and disease risk. Research on BAT and WAT now focuses on their roles in obesity and related metabolic diseases [1–3]. Obesity results from an energy imbalance, with

WAT expansion, especially visceral fat, linked to higher risks of type 2 diabetes, cardiovascular disease, and other conditions [4–6]. BAT, due to its ability to burn energy, is considered a potential target for obesity treatment.

The transition between BAT and WAT, particularly the “browning” of WAT, can be triggered by cold exposure and exercise. Conversely, factors like environment, nutrition, and hormones, especially glucocorticoids, influence the “whitening” of BAT [7–9]. Glucocorticoids, stress-response hormones, can lead to increased WAT and reduced BAT function, lowering thermogenic capacity and raising the risk of metabolic disorders like obesity and diabetes [10]. Most research in this area has been on rodents, but rabbits, which share similar brown fat development with humans, are a suitable model.

*Correspondence:

Xiuzhu Sun
sunxiuzhu@nwfau.edu.cn

Shuhui Wang
wangshuhui@nwfau.edu.cn

¹College of Animal Science and Technology, Northwest A&F University, Yangling, Shaanxi 712100, P. R. China

²College of Grassland Agriculture, Northwest A&F University, Yangling, Shaanxi 712100, P. R. China



© The Author(s) 2025. **Open Access** This article is licensed under a Creative Commons Attribution-NonCommercial-NoDerivatives 4.0 International License, which permits any non-commercial use, sharing, distribution and reproduction in any medium or format, as long as you give appropriate credit to the original author(s) and the source, provide a link to the Creative Commons licence, and indicate if you modified the licensed material. You do not have permission under this licence to share adapted material derived from this article or parts of it. The images or other third party material in this article are included in the article's Creative Commons licence, unless indicated otherwise in a credit line to the material. If material is not included in the article's Creative Commons licence and your intended use is not permitted by statutory regulation or exceeds the permitted use, you will need to obtain permission directly from the copyright holder. To view a copy of this licence, visit <http://creativecommons.org/licenses/by-nc-nd/4.0/>.

This study explored how dexamethasone (Dex), a glucocorticoid, affects BAT in rabbits, both in vivo and in vitro. Clinically, this helps deepen understanding of metabolic diseases, and in livestock, it suggests potential ways to maintain higher metabolic rates by preventing the whitening of BAT. Ultimately, identifying the molecular mechanisms behind glucocorticoid-induced BAT whitening could aid in developing therapies to improve energy balance and metabolic health.

Materials and methods

Animal treatment

Experimental rabbits were obtained from the Tianxin Rabbit Breeding Factory in Yangling, Shaanxi Province. For this study, 7-day-old male rabbits, primarily weighing 80 g, were randomly allocated to various treatment groups ($n=8$). Rabbits in the experimental group were intraperitoneally injected with dexamethasone sodium phosphate (Huaxu Biotech, Henan, China) at a dose of 5 mg/kg per day for one week. Rabbits in the control group received an equivalent volume of normal saline following the same treatment schedule. Body weight was recorded daily. At the end of the treatment period, the rabbits were euthanized via cervical dislocation, and samples of interscapular brown adipose tissue (iBAT), dorsal brown adipose tissue (dBAT), subcutaneous white adipose tissue (sWAT) and perirenal adipose tissue (PAT) were collected and stored at -80°C .

RNA extraction and quantitative Real-Time PCR (qRT-PCR)

Total RNA was extracted from brown adipose tissue and adipocytes using TRIzol™ reagent (Thermo Fisher Scientific, Waltham, MA, USA), and RNA integrity was resolved using a NanodropnD-100 spectrophotometer (2000 C, Thermo Fisher Scientific, Waltham, MA, USA) and 1% agarose gel electrophoresis. A complementary DNA (cDNA) template was synthesized using the Fast-King gDNA Dispelling RT SuperMix Kit (Tiangen Biotech, Beijing, China). qRT-PCR assays were conducted using a CFX Connect system (Bio-Rad, CA, USA) with a total reaction volume of 20 μL consisting of SYBR Green SuperReal PreMix Plus (Tiangen Biotech, Beijing, China). This mixture included 7.5 μL of SYBR Green, 0.4 μL of both forward and reverse primers (10 $\mu\text{mol/L}$), 1 μL of cDNA template, and 5.7 μL of RNase-free ddH₂O. The PCR conditions were as follows: predenaturation at 95°C for 15 min; 35 cycles of denaturation at 95°C for 10 s, annealing at 55°C for 30 s, and extension at 72°C for 32 s; and 95°C for 15 s and 65°C for 5 s. The relative expression of the target gene was normalized to that of β -actin and calculated using the $2^{-\Delta\Delta\text{Ct}}$ method [11].

Primary culture of brown adipocytes

Adipocytes were isolated from brown adipose tissue obtained from the interscapular region of five 1-day-old rabbits using the collagenase digestion method (Solarbio, Beijing, China, Cat. No. GC305014). Briefly, the adipose tissue was rinsed in phosphate-buffered saline (PBS) containing 4% penicillin-streptomycin (Solarbio, Beijing, China, Cat. No. P1400) and then placed in a 0.1% collagenase type II solution at 37°C for 1 h. Thereafter, the solution was filtered through a 200-mesh cell sieve, and the cells (5×10^4) were inoculated in DMEM/F12 (Solarbio, Beijing, China, Cat. No. D6570) containing 10% fetal bovine serum (FBS) (Solarbio, Beijing, China, Cat. No. 11011-8611) and cultured at 37°C under a 5% CO₂ atmosphere. The culture medium was replaced every 48 h. Subsequently, adipocytes were treated with Dex (Solarbio, Beijing, China, Cat. No. 50-02-2) to assess the effects.

HE staining, immunohistochemistry staining and transmission Electron microscopy (TEM)

The adipose tissue was fixed in adipose fixation solution (Sercivebio, Wuhan, China, Cat. No. G1119) prior to HE staining and immunohistochemistry (UCP1, Sercivebio, Wuhan, China, Cat. No. GB112174) analysis. The brown adipose tissue was cut into 1–3 mm squares, fixed in 4% glutaraldehyde (Sercivebio, Wuhan, China, Cat. No. G1102) for 1 h at room temperature and left at 4°C overnight for TEM. HE staining, immunohistochemistry and TEM were performed by Sercivebio Biotech Co., Ltd. To quantitatively analyze UCP1 protein expression from immunohistochemical images using ImageJ, images were captured with consistent exposure settings to minimize bias and then converted to 8-bit grayscale for easier thresholding. A uniform threshold was applied across all images to isolate the brown-stained areas indicative of positive UCP1 expression from the background. The “Analyze Particles” function was used to calculate the area of positive staining, excluding small particles to avoid non-specific signals. The percentage of positive area was determined by dividing the total positive staining area by the total region of interest (ROI) area. For each sample, multiple ROIs were analyzed, and at least three sections were examined to account for variability. Statistical tests were then applied to compare UCP1 expression levels among different groups, ensuring a reliable and reproducible quantification.

CCK-8 cell proliferation assay

The CCK-8 (Cell Counting Kit-8) assay was used to assess cell proliferation and viability. Cells were seeded in 96-well plates at 5000 cell/well densities and incubated under standard culture conditions for 24 h to allow cell adhesion. After cell attachment, cells were treated with

different concentrations of the Dex or control treatments and incubated for 24 h. After treatment, 10 μ L of CCK-8 reagent (Seven, Beijing, China, Cat. No. SC119) was added to each well and incubated for an additional 1–4 h at 37 °C. The absorbance at 450 nm was measured using a microplate reader to quantify cell proliferation. Cell viability or proliferation was calculated based on the absorbance values and normalized to the control group.

Oil red O staining

Oil Red O staining was used to assess adipocyte differentiation by visualizing lipid accumulation in the cells. Cells were cultured and induced to differentiate in adipogenic induction medium for 10 days. After differentiation, cells were washed with PBS and fixed with 4% paraformaldehyde (PFA) for 30 min at room temperature. The fixed cells were washed with PBS and stained with freshly prepared Oil Red O solution (Sercivebio, Wuhan, China, Cat. No. G1262) for 30 min at room temperature. Excess dye was removed by washing the cells with distilled water. Images were captured under a microscope to assess lipid droplet accumulation. To quantify the Oil Red O staining, the dye was eluted with isopropanol, and the absorbance was measured at 490 nm using a microplate reader.

ATP content measurement

The ATP content in brown adipocytes was measured using a commercially available ATP assay kit (Sangon Biotech, D799643-0050) following the manufacturer's protocol. Cells were collected and lysed, and the ATP content was quantified using a UV spectrophotometer at 340 nm, based on the generation of NADPH, which is proportional to the ATP concentration. The results were normalized to cell count, and data are expressed as μ mol of ATP per 10^6 cells.

RNA sequencing and data analysis

The process of RNA sequencing includes RNA extraction, RNA detection, library construction, and upsequencing. RNA sequencing analysis was performed on the iBAT of rabbits ($n=3$ for the control group and Dex group). Briefly, RNA purity was checked using a NanoPhotometer[®] spectrophotometer (IMPLEN, CA, United States). Then, the RNA concentration was measured using a Qubit[®] RNA Assay Kit in a Qubit[®] 2.0 Fluorometer (Life Technologies, CA, United States). After that, RNA integrity was assessed using the RNA Nano 6000 Assay Kit of the Bioanalyzer 2100 system (Agilent Technologies, CA, United States). Library preparations were sequenced on the Illumina HiSeq platform, and 125/150 bp double-end reads were generated. The raw read quality was assessed using FastQC (v0.11.5). STAR (v2.7.3a) was used to align the reads to the rabbit genome (UM_NZW_1.0). Transcript quantification was performed using featureCounts

in paired-end mode to count both uniquely mapped reads. Differentially expressed genes were called using edgeR (v2.26.5) with Benjamini–Hochberg adjusted P value < 0.01 and $\log_2|\text{FoldChange}| > 1.5$. The R package clusterProfiler (v4.6.1) was utilized for gene set enrichment analysis. The gene set matrix was prepared using createSet in GSEA, and enrichment analysis was performed with runGSEA, plotting results with the GSEA plot function to show NESs and other metrics. R plotting functions help visualize differentially expressed genes and enriched sets.

LEPR overexpression and inhibition

To construct a plasmid for the overexpression of the leptin receptor (*LEPR*), we utilized the pCMV-*LEPR*-3xFLAG-Neo plasmid. The *LEPR* coding sequence was cloned and inserted into the pCMV vector, generating the overexpression plasmid. Once the cells reached the appropriate confluency, the pCMV-*LEPR*-3xFLAG-Neo overexpression plasmid was introduced into primary brown adipocytes using Lipo8000 (Beyotime, Shanghai, China, Cat. No. C0533), ensuring efficient cellular uptake and expression of the plasmid. Transfection with empty vector was performed as control group. Following transfection, the cells were incubated for 24 h to allow for the expression of the *LEPR* gene.

LEPR siRNA was designed and synthesized by Sangon Biotech, and a non-targeting siRNA was used as a negative control. Cells were seeded in 6-well plates at approximately 70–80% confluency for transfection. Transfection was carried out using Lipo8000 (Beyotime, Shanghai, China, Cat. No. C0533) according to the manufacturer's protocol. siRNA (final concentration of 50 nM) was mixed with Lipo8000 in serum-free medium and incubated at room temperature for 15 min to allow complex formation. The siRNA-Lipofectamine complexes were added to the cells and gently mixed. Cells were incubated for 24 h under standard culture conditions.

The experiment was divided into four groups: the control group, which received no treatment; the Dex group, which was treated with 10 μ M Dex for 24 h; the empty vector + Dex group (or si-NC + Dex) where cells were first transfected with an empty vector plasmid (or si-NC) for 24 h and then treated with 10 μ M Dex for another 24 h; and the over-*LEPR* + Dex group (or si-*LEPR* + Dex), where cells were first transfected with an *LEPR* overexpression plasmid (or si-*LEPR*) for 24 h and then treated with 10 μ M Dex for another 24 h.

Transfection efficiency was assessed by qRT-PCR to measure *LEPR* mRNA levels. Total RNA was extracted from each group of cells, reverse-transcribed into cDNA using a reverse transcription kit, and qRT-PCR was performed using SYBR Green PCR Master Mix to detect the relative expression levels of target genes, including *LEPR*,

PGC1A, *PRDM16*, *UCP1*, and *PPARG*, with β -actin as the internal reference gene.

Statistical analysis

The data are presented as the means \pm SDs and were analysed using a t test and one-way analysis of variance (ANOVA) for group comparisons. HE staining and TEM analyses were conducted using ImageJ version 1.53. Statistical analyses were carried out with GraphPad Prism software (version 8.0.2). $P < 0.05$ was considered to indicate statistical significance.

Results

Dex increases brown adipose tissue mass and results in white adipose tissue characteristics

Dex was observed to increase the mass of BAT and induce the acquisition of white adipose tissue in rabbits. The BAT in rabbits primarily comprises interscapular iBAT and dBAT. Dex treatment resulted in a reduced rate of weight gain compared to the control group (Fig. 1A, B), while the relative weights of both the iBAT and dBAT markedly increased. In contrast, the relative weights of sWAT and PAT decreased significantly (Fig. 1C). HE staining revealed that the adipocytes in the dBAT and iBAT transitioned from multilocular to unilocular lipid droplets following Dex administration (Fig. 1D), with the dBAT showing a heterogeneous transition, progressively shifting from multilocular to unilocular lipid droplets in a centrifugal pattern. This pattern may indicate a progressive ‘whitening’ of brown adipose tissue from the core to the periphery. Furthermore, ultrastructural analysis of iBAT revealed an increase in the lipid droplet area and a concurrent decrease in the mitochondrial count (Fig. 1E), suggesting potential impairment of the mitochondrial function of brown adipose tissue.

Dex impacts thermogenic gene and protein expression in iBAT. The expression of the thermogenic gene *UCP1* was assessed using RT-qPCR and immunohistochemistry (IHC). IHC results indicated that UCP1 positivity was significantly lower in the Dex-treated group than in the control group, as shown in Fig. 1F. However, the *UCP1* mRNA levels in the Dex group did not show significant changes (Fig. 1G). These results are based on the gene mRNA level per mg RNA. Since the mass of brown adipose tissue increased after Dex treatment, we believe this may have diluted the UCP1 expression per unit mass. From a whole-animal perspective, the thermogenic capacity of brown adipose tissue may not have changed significantly. The inconsistency between UCP1 mRNA and protein levels could be due to differences in their half-lives.

Dex inhibited thermogenesis in primary brown adipocytes and promoted their proliferation and differentiation

To assess the effects of Dex, primary brown adipocytes were exposed to various concentrations of Dex (0, 1, 5, or 10 μ M) for 48 h. Posttreatment, the expression levels of the thermogenesis-related genes *UCP1*, *PGC1A*, *DIO2*, and *PRDM16* decreased, whereas *PPARG* and *LPL* expression increased (Fig. 2A). Direct measurement of ATP content in response to Dex treatment demonstrated a dose-dependent decrease in ATP levels, providing direct evidence of Dex’s impact on mitochondrial energy production in brown adipose tissue (Fig. 2B). A cell proliferation assay using a CCK-8 kit demonstrated that 10 μ M Dex enhanced adipocyte proliferation (Fig. 2C). Adipogenic differentiation, assessed by oil red O staining, indicated a concentration-dependent increase in adipogenic potential in response to Dex (Fig. 2D).

Transcriptome characterization of rabbit brown adipose RNA-seq

Subsequent RNA-seq analysis of rabbit iBAT revealed 1,270 differentially expressed genes (DEGs) between the control and Dex groups, with 318 upregulated and 952 downregulated genes (Fig. 3A, B). The cut-off for differential expression was set at $|\text{fold change}| > 1.5$. Principal component analysis distinctly separated the control and Dex groups into two clusters, providing valuable insights for further analysis (Fig. 3C). Functional enrichment analysis revealed that the DEGs were primarily involved in autophagy, *PPARG* signalling pathways, and other brown adipose-related metabolic processes. Furthermore, DEGs were significantly enriched in pathways related to myocardial contraction and gastric acid secretion, indicating that glucocorticoids affect the body (Fig. 3D, E). Gene Set Enrichment Analysis (GSEA) highlighted a reduction in the PI3K-Akt and NF-Kappa B signalling pathway. (Fig. 3F). However, there was no change in the mitochondrial membrane potential after Dex treatment in brown adipocytes (Fig. S1).

BAT and WAT showed distinct changes, and the weights of sWAT and PAT decreased following Dex treatment. Histological analysis revealed no significant change in adipocyte size in sWAT but a marked reduction in adipocyte size in PAT (Fig. S2A). RNA sequencing of sWAT highlighted DEG enrichment in pathways such as oxidative phosphorylation, fatty acid metabolism, and the synthesis of steroid hormones (Fig. S2C). The decline in the PPAR pathway suggested a shift towards enhanced lipid breakdown, contrasting with the BAT findings and implicating altered fat metabolism in various metabolic disorders.

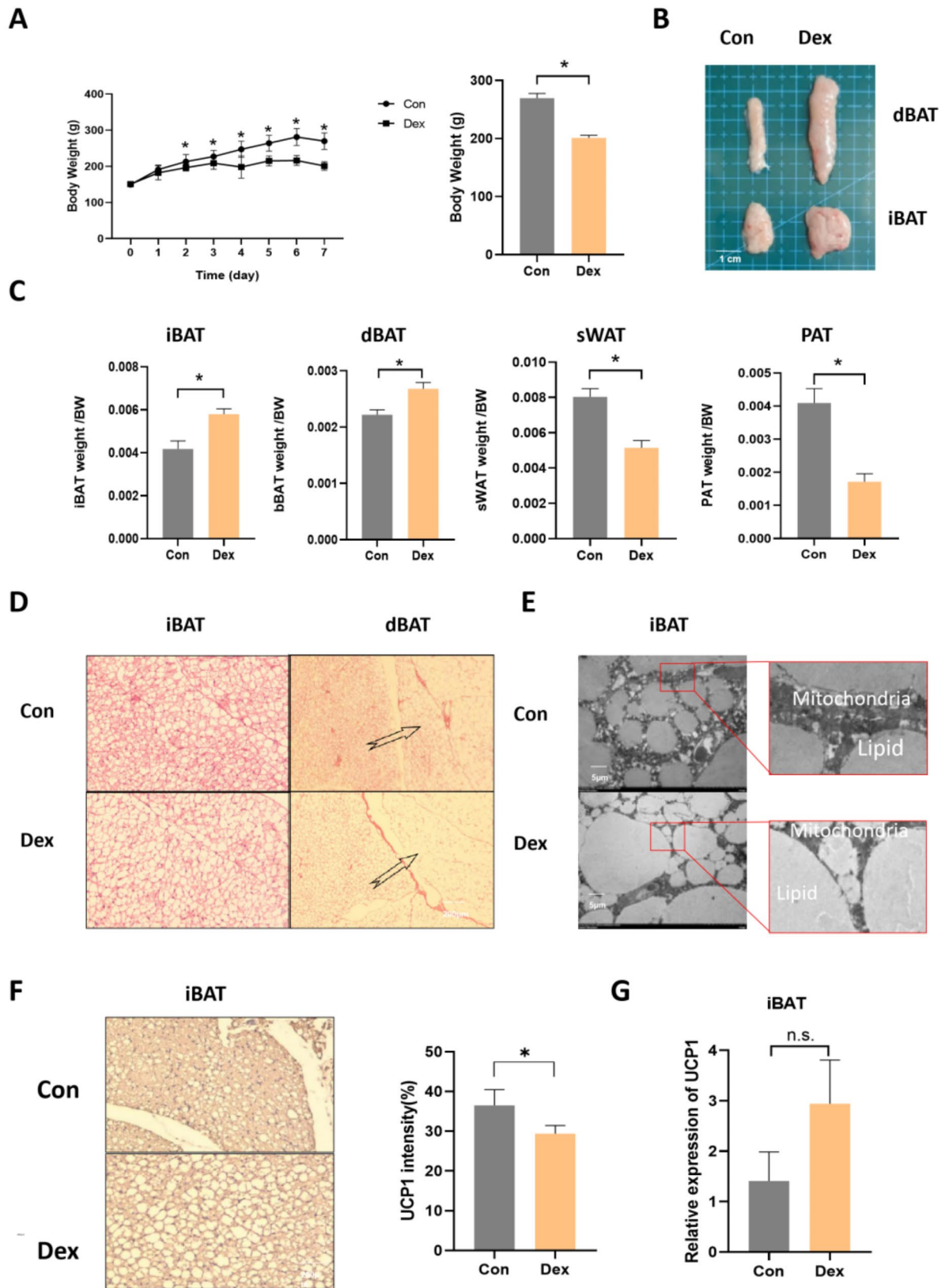
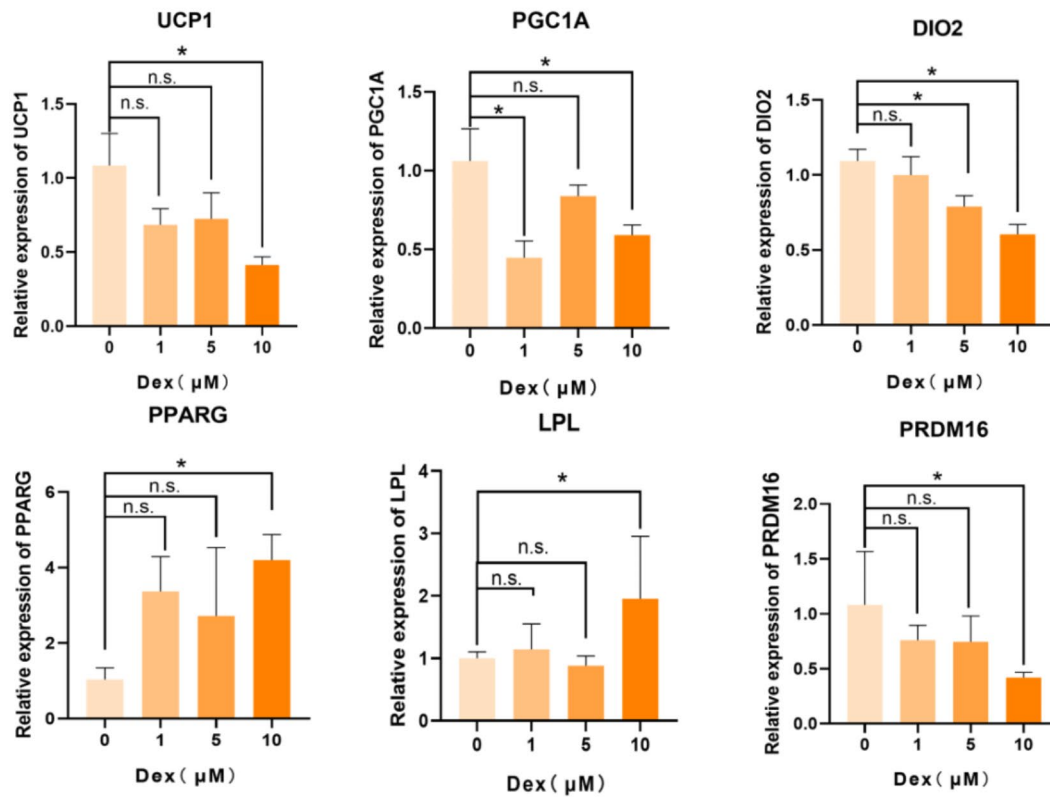
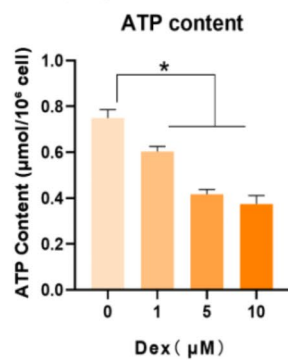


Fig. 1 Weight, morphology and histological structure of rabbit adipose tissue and expression of thermogenic gene and protein. **A.** Weekly weight changes in rabbits. **B.** Morphology of the iBAT and dBAT. **C.** Weight indices of BAT and WAT. **D.** HE staining of the iBAT and dBAT. **E.** Transmission electron microscopy of iBAT. * $P < 0.05$. Arrow: Direction of BAT whitening. **F.** UCP1 immunohistochemistry. **G.** UCP1 mRNA expression. * $P < 0.05$

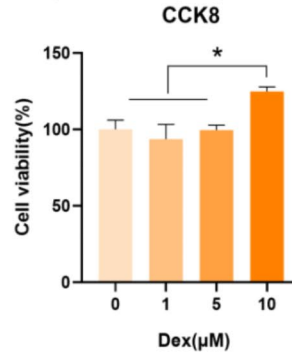
A Primary brown adipocytes



B Primary brown adipocytes



C Primary brown adipocytes



D

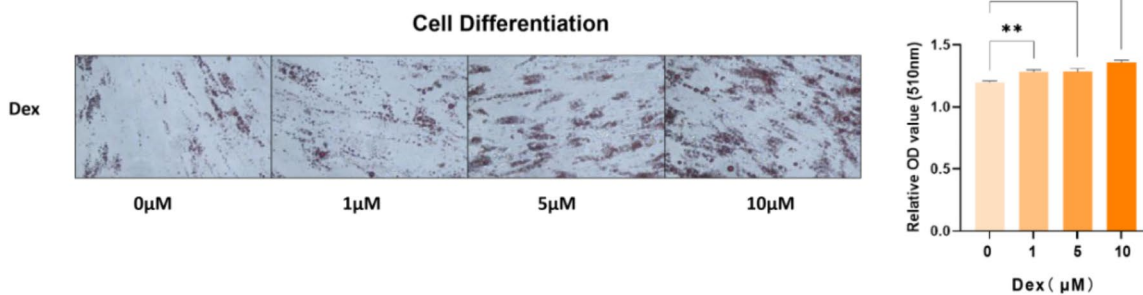


Fig. 2 Effects of Dex treatment on gene expression, cell proliferation, and cell differentiation in brown adipocytes. **A.** Thermogenic and fat metabolism gene expression. **B.** ATP content in primary brown adipocyte. **C.** Primary brown adipocyte proliferation. **D.** Primary brown adipocyte differentiation. **P* < 0.05, ***P* < 0.01, *****P* < 0.0001

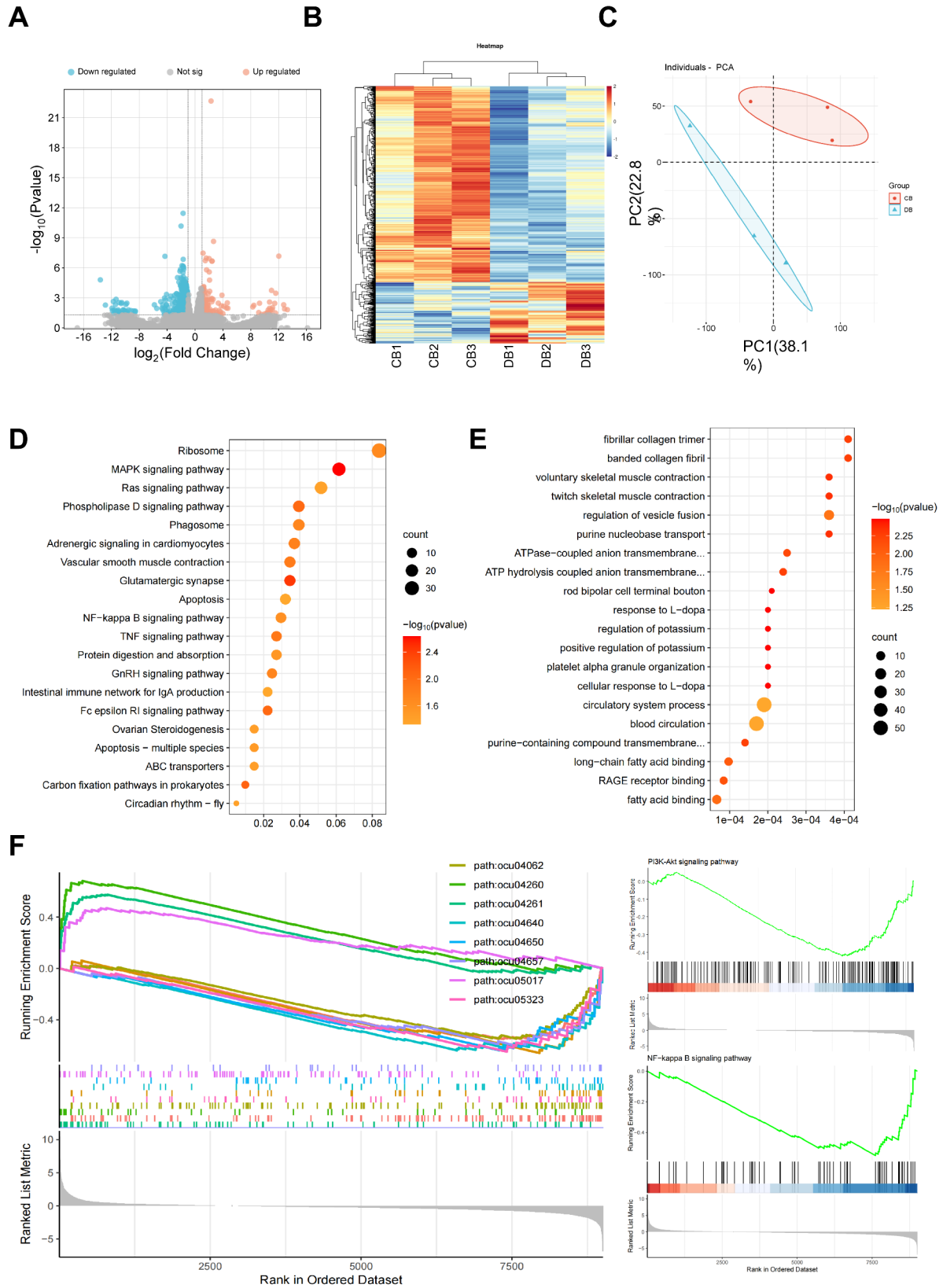


Fig. 3 RNA-seq characterization of iBAT. **A.** Volcano plot. **B.** Heatmap of DEGs. **C.** Principal Component Analysis (PCA) plot. **D.** Top 20 KEGG pathway analysis of DEGs. **E.** Top 20 GO term analysis of DEGs. **F.** GSEA

Dex inhibited thermogenesis and decreased the oxidation of fatty acids

Based on the transcriptome sequencing results, we analysed the expression levels of genes associated with mitochondria, fatty acid oxidation and markers in both white and brown adipose tissue. The results showed that the expression of *CYTB*, *OPA1*, *MFN1*, *COX3*, *ATP6*, *CPT1*, *ACADM*, *SREBF* and *PGC1A* decreased in the Dex group, while that of the white adipose tissue marker *LEP* increased (Fig. 4). Our findings revealed that Dex treatment resulted in significant downregulation of mitochondrial functional genes and inhibition of fatty acid oxidation. Furthermore, brown adipose marker genes exhibited a significant reduction in expression. The expression of the white lipid differentiation marker gene leptin increased significantly, and the primary source of leptin was white adipose tissue. Concurrently, the decrease in *LEPR* levels led us to speculate that leptin resistance may occur in this process. In essence, while leptin is known to combat obesity, its efficacy might be limited by its receptor.

LEPR overexpression reverses Dex-Induced downregulation of mitochondrial biogenesis gene expression

To investigate the role of *LEPR* in Dex-induced metabolic disturbances and impaired thermogenesis in brown adipocytes, we first examined the dose-dependent effects of Dex on *LEP* and *LEPR* expression (Fig. 5A). qRT-PCR analysis showed that Dex treatment significantly increased *LEP* expression in a dose-dependent manner, with a significant difference observed at 10 μ M ($P < 0.05$), while *LEPR* expression was downregulated at higher Dex concentrations. To further investigate whether *LEPR* modulates Dex-induced whitening, we overexpressed and knocked down *LEPR* in primary brown adipocytes. The qRT-PCR results confirmed that transfection with the *LEPR* overexpression plasmid significantly increased *LEPR* mRNA levels ($P < 0.05$), whereas transfection with siRNA significantly reduced *LEPR* expression ($P < 0.05$), verifying the success of both approaches. In brown adipocytes, Dex treatment significantly downregulated *LEPR* expression ($P < 0.05$). Compared to the empty vector control, *LEPR* overexpression (+*LEPR*) significantly increased *LEPR* expression ($P < 0.05$), confirming the effectiveness of the overexpression strategy. Under Dex

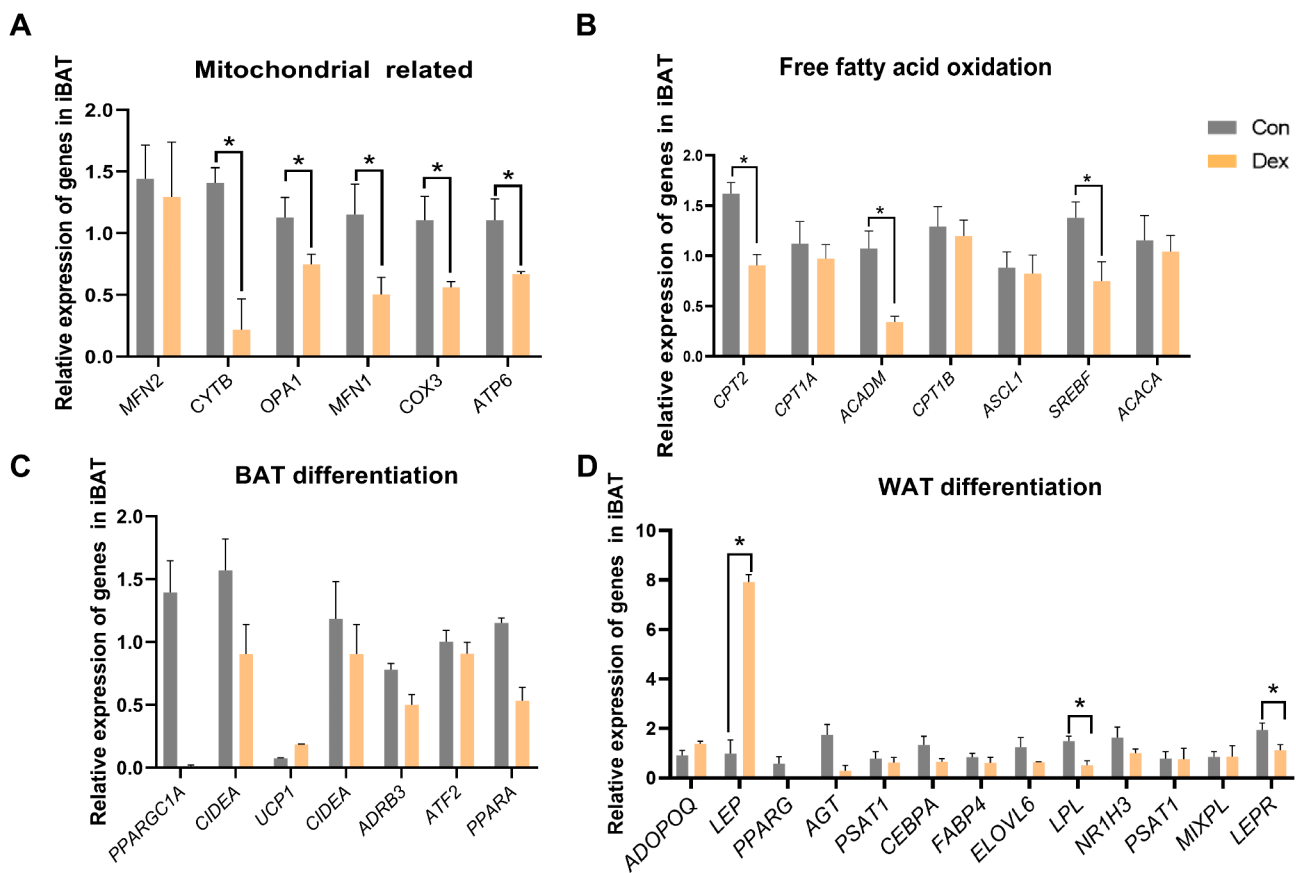
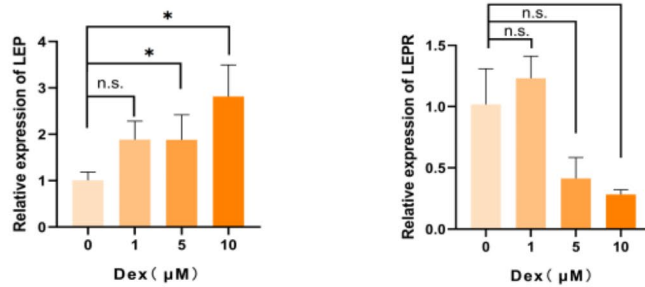
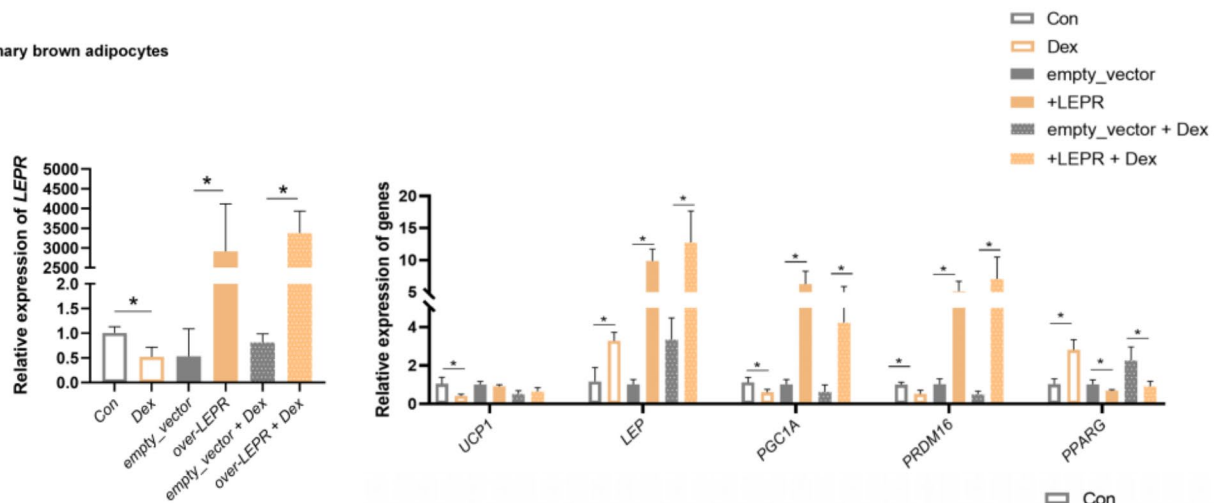


Fig. 4 Expression of genes related to fat metabolism. **A.** Mitochondrial-related gene expression. **B.** Fatty acid oxidation-related genes. **C.** BAT differentiation-related genes. **D.** WAT differentiation-related genes. * $P < 0.05$

A Primary brown adipocytes



B Primary brown adipocytes



C Primary brown adipocytes

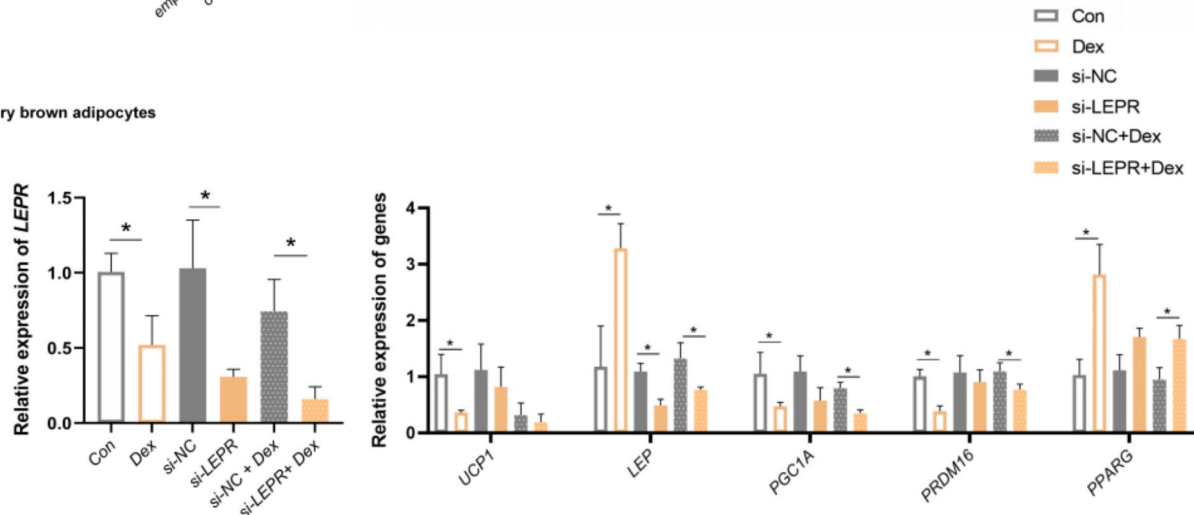


Fig. 5 Role of *LEPR* in Dex-treated brown adipocytes. **A.** Effects of Dex treatment on *LEP* and *LEPR* gene expression in primary brown adipocytes. **B.** Quantification of *LEPR* overexpression efficiency and expression of mitochondrial and thermogenic genes after *LEPR* overexpression. **C.** Quantification of *LEPR* inhibition efficiency and expression of mitochondrial and thermogenic genes after *LEPR* inhibition in Dex group, * $P < 0.05$

treatment, *LEPR* expression was partially restored in the +*LEPR*+Dex group ($P < 0.05$), suggesting that *LEPR* overexpression may mitigate Dex-induced suppression of *LEPR* expression. We next examined whether *LEPR* modulates genes associated with thermogenesis and adipocyte differentiation. As expected, Dex treatment significantly reduced the expression of *UCP1*, *PGC1A*, and *PRDM16*

($P < 0.05$), while significantly upregulating *PPARG* ($P < 0.05$), confirming that Dex promotes brown adipose whitening. Notably, *LEPR* overexpression (+*LEPR*+Dex) partially restored *UCP1*, *PGC1A*, and *PRDM16* expression levels ($P < 0.05$) while significantly reducing *PPARG* expression ($P < 0.05$), suggesting that *LEPR* overexpression can partially counteract Dex-induced whitening

(Fig. 5B). Conversely, *LEPR* knockdown (*si-LEPR*) significantly increased *PPARG* expression ($P < 0.05$), indicating that *LEPR* deficiency may enhance adipocyte differentiation toward a white fat phenotype. *PGC1A* expression was also slightly reduced in the *si-LEPR* group, but the change was not statistically significant compared to *si-NC*, suggesting that the regulation of mitochondrial biogenesis by *LEPR* may require additional factors or Dex stimulation. *PRDM16* expression did not show significant changes in the *si-LEPR* group compared to *si-NC*, further suggesting that *PRDM16* suppression is primarily dependent on Dex rather than *LEPR* loss alone.

However, in the *si-LEPR*+Dex group, *PRDM16* expression was significantly downregulated ($P < 0.05$), alongside continued suppression of *PGC1A* and further upregulation of *PPARG*. These results suggest that *LEPR* knockdown enhances Dex-induced adipogenic differentiation while having a minimal additional impact on mitochondrial biogenesis and thermogenic gene suppression in the absence of Dex. However, under Dex treatment, the loss of *LEPR* exacerbates the downregulation of *PRDM16* and other thermogenic genes, further promoting the whitening phenotype of brown adipocytes (Fig. 5C).

Together, these findings suggest that while *LEPR* plays a crucial role in modulating adipocyte differentiation through *PPARG* and mitochondrial biogenesis via *PGC1A*, its influence on thermogenic gene expression, such as *PRDM16*, is more dependent on Dex-induced mechanisms rather than *LEPR* loss alone. The consistency of these results with Dex treatment further supports *LEPR* as a key modulator of brown adipose plasticity.

Discussion

This study was an exploration of the effects of glucocorticoids, specifically Dex, on the metabolic transition of BAT to WAT. We observed a notable shift towards a white adipose phenotype in the rabbit model, characterized by increased lipid deposition, reduced mitochondrial density and altered expression of thermogenic and mitochondrial markers. These findings align with observations in rodent models treated with glucocorticoids, demonstrating similar adipose tissue remodelling [12–16]. After treatment with Dex, the expression levels of genes related to mitochondrial function (such as *CYTB*, *OPA1*, *MFN1*, *COX3*, *ATP6*) significantly decreased. Additionally, the ATP content in adipocytes showed a concentration-dependent decline with Dex, further indicating impaired mitochondrial biogenesis and function. The expression levels of genes involved in fatty acid oxidation (such as *CPT1*, *ACADM*) also decreased, suggesting that fatty acid oxidation was inhibited. Additionally, we determined the direct effect of Dex on brown adipocytes by measuring cellular ATP levels.

Interestingly, while a decrease in *UCP1* expression was noted in Dex-treated brown adipocytes, the BAT showed no significant change in *UCP1* expression post-Dex treatment. These results are based on the gene mRNA level per mg RNA. Since the mass of brown adipose tissue increased after Dex treatment, we believe this may have diluted the *UCP1* expression per unit mass. From a whole-animal perspective, the thermogenic capacity of brown adipose tissue may not have changed significantly. The inconsistency between *UCP1* mRNA and protein levels could be due to differences in their half-lives, with *UCP1* mRNA having a relatively shorter half-life. This contradicts the conventional belief that glucocorticoids primarily induce lipid accumulation and diminish BAT thermogenic function [17–19]. Previous studies have shown Dex-induced *UCP1* reduction appeared only under thermoneutral conditions, implying that external factors may affect *UCP1* expression and BAT activation [20].

Studies have shown that autophagic degradation of mitochondria appears to be important for the inactivation of brown fat and the transition from beige to white adipose tissue. Our study also highlighted the importance of autophagy and mitophagy [9]. Deng et al. reported that glucocorticoids induce significant whitening of BAT via BTG1- and ATG7-dependent autophagy [13]. RNA-seq analysis further confirmed an increase in autophagy pathways, with increased expression of the mitophagy markers *PINK1* and *LC3II*. However, no significant effect of Dex on the mitochondrial membrane potential was detected, possibly reflecting physiological differences between in vivo and in vitro settings [21–25].

Glucocorticoids increase lipid synthesis and storage [26]. In BAT, Dex promotes the accumulation of lipid droplets within fat cells. The main function of BAT is to consume energy through thermogenesis, a process that is highly dependent on the function of mitochondria [27–29]. Dex reduces the number and function of mitochondria, leading to a reduction in the energy expenditure of BAT, thus promoting energy storage. Dex may affect mitochondrial biosynthesis and degradation processes, leading to a decrease in mitochondrial numbers. This effect may be related to a glucocorticoid-induced increase in mitochondrial autophagy or downregulation of mitochondrial biosynthesis [30].

Research indicates that glucocorticoids affect lipid metabolism by increasing lipolysis in certain adipose depots while simultaneously increasing lipid accumulation in others [10, 31]. In rabbits, this dual action facilitates the redistribution of body fat and alterations in the lipid profile, potentially explaining why brown and white adipose tissues exhibit completely different phenotypes and fat metabolism characteristics.

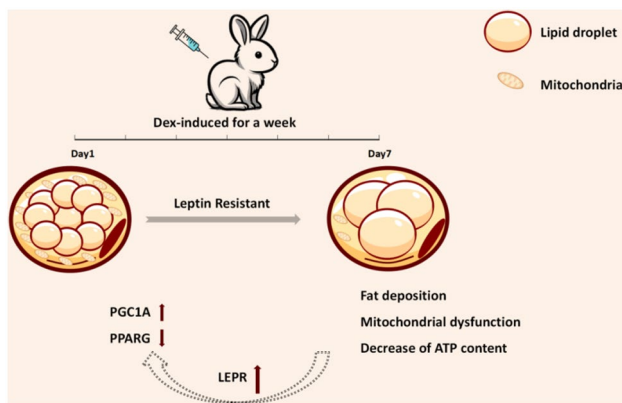


Fig. 6 Summary Graph

The glucocorticoid-driven changes in adipokine secretion, characterized by elevated leptin and increased adiponectin, may exacerbate metabolic imbalance, paving the way for obesity and insulin resistance [32]. In particular, the downregulation of *LEPR* in BAT prompted speculation about leptin resistance, which is a critical area for further exploration. If there is leptin resistance or a decrease in leptin receptor expression, even with elevated leptin levels, it cannot exert its physiological effects [33]. Therefore, we hypothesize that glucocorticoid-induced leptin resistance in brown adipocyte leads to the downregulation of key genes involved in mitochondrial biogenesis and thermogenesis, as well as alterations in lipid metabolism. Our results showed that Dex-induced thermogenesis inhibition was not fully reversed by *LEPR* overexpression in primary brown adipocytes. However, the overexpression of *LEPR* did modulate the expression of *PGC1A* and *PPARG*, which are important regulators of mitochondrial biogenesis and energy metabolism. Conversely, the inhibition of *LEPR* further reversed the expression of these genes, highlighting the role of leptin resistance in mediating mitochondrial function. Therefore, addressing other aspects of glucocorticoid signaling pathways may be necessary to fully mitigate the adverse effects on thermogenesis and energy metabolism, highlighting the need for further research into the complex interactions between glucocorticoids and BAT function (Fig. 6).

In this study, we employed Dex concentrations that exceed typical physiological and clinical levels. These supraphysiological doses were chosen based on previous studies to investigate the maximal effects of glucocorticoids on adipose tissue. While the experiments with *LEPR* silencing in the absence of Dex provide important insights into leptin signaling, the inclusion of Dex treatment allows us to model stress-induced metabolic changes in adipose tissue. This combination further clarifies the mechanistic role of *LEPR* under glucocorticoid exposure and strengthens the conclusions drawn from

our study. However, this approach has its limitations. Future studies should focus on investigating the effects of Dex at concentrations more representative of therapeutic doses to better align the findings with clinical practice and further validate the observed mechanisms. Moreover, this investigation not only provides insights into glucocorticoid-induced fat redistribution in animal husbandry but also has broader implications for understanding the contributions of glucocorticoids to obesity and metabolic diseases in mammals.

Abbreviations

Dex	Dexamethasone
BAT	Brown adipose tissue
WAT	White adipose tissue
UCP1	Uncoupling protein-1
iBAT	interscapular brown adipose tissue
dBAT	dorsal brown adipose tissue
sWAT	subcutaneous white adipose tissue
PAT	Perirenal adipose tissue
LEPR	Leptin Receptor
DEGs	Differentially expressed genes
GSEA	Gene set enrichment analysis
PCA	Principal component analysis
TEM	Transmission electron microscopy

Supplementary Information

The online version contains supplementary material available at <https://doi.org/10.1186/s12864-025-11502-3>.

Supplementary Material 1
 Supplementary Material 2
 Supplementary Material 3
 Supplementary Material 4
 Supplementary Material 5
 Supplementary Material 6
 Supplementary Material 7
 Supplementary Material 8
 Supplementary Material 9

Acknowledgements

Not applicable.

Author contributions

XT: Writing– review & editing, Writing– original draft. BZ: Cell culture and Investigation. PX: Samples collection and qRT-PCR. YW: Cell culture. YQ: Data curation. XY: Samples collection. ZZ: Samples collection. MS: Samples collection. XS: Experimental design. SW: Experimental design.

Funding

This work was funded by the Key R & D Plan Projects in Shaanxi Province: Integration and demonstration of rabbit breed breeding and factory reproduction technology (2018ZDXM-NY-041), and the Shaanxi Province Agricultural Science and Technology Innovation Special Fund Project: Using Multi-omics techniques to improve rabbit meat performance and cultivate new varieties (20231494).

Data availability

The datasets generated and/or analysed during the current study are available in the NCBI repository (<https://www.ncbi.nlm.nih.gov/bioproject/PRJNA1098965>).

Declarations**Ethics approval and consent to participate**

All experimental procedures were performed in accordance with the Regulations for the Administration of Affairs Concerning Experimental Animals approved by the State Council of People's Republic of China. The study was approved by the Institutional Animal Care and Use Committee of Northwest A&F University (Permit Number: NWAFA1019).

Consent for publication

Not applicable.

Competing interests

The authors declare no competing interests.

Received: 21 May 2024 / Accepted: 19 March 2025

Published online: 31 March 2025

References

- Fenzl A, Kiefer FW. Brown adipose tissue and thermogenesis. *Horm Mol Biol Clin Investig.* 2014;19(1):25–37.
- Hachemi I, U-Din M. Brown adipose tissue: activation and metabolism in humans. *Endocrinol Metab (Seoul).* 2023;38(2):214–22.
- Feng X, Wang L, Zhou R, Zhou R, Chen L, Peng H, Huang Y, Guo Q, Luo X, Zhou H. Senescent immune cells accumulation promotes brown adipose tissue dysfunction during aging. *Nat Commun.* 2023;14(1):3208.
- Reyes-Farías M, Fos-Domenech J, Serra D, Herrero L, Sánchez-Infantes D. White adipose tissue dysfunction in obesity and aging. *Biochem Pharmacol.* 2021;192:114723.
- Cheng L, Wang J, Dai H, Duan Y, An Y, Shi L, Lv Y, Li H, Wang C, Ma Q, et al. Brown and beige adipose tissue: a novel therapeutic strategy for obesity and type 2 diabetes mellitus. *Adipocyte.* 2021;10(1):48–65.
- Carpentier AC, Blondin DP, Haman F, Richard D. Brown adipose Tissue—A translational perspective. *Endocr Rev.* 2023;44(2):143–92.
- Nirengi S, Stanford K. Brown adipose tissue and aging: A potential role for exercise. *Exp Gerontol.* 2023;178:112218.
- Lehning AC, Stanford KI. Exercise-induced adaptations to white and brown adipose tissue. *J Exp Biol* 2018, 221(Pt Suppl 1).
- Ziqubu K, Dlodla PV, Mthembu SXH, Nkambule BB, Mabhidha SE, Jack BU, Nyambuya TM, Mazibuko-Mbeje SE. An insight into brown/beige adipose tissue whitening, a metabolic complication of obesity with the multifactorial origin. *Front Endocrinol.* 2023;14:114767.
- Peckett AJ, Wright DC, Riddell MC. The effects of glucocorticoids on adipose tissue lipid metabolism. *Metab Clin Exp.* 2011;60(11):1500–10.
- Livak KJ, Schmittgen TD. Analysis of relative gene expression data using real-time quantitative PCR and the 2⁻(Delta delta C(T)) method. *Methods.* 2001;25(4):402–8.
- Assis AP, Silva KE, Lautherbach N, Morgan HJN, Garófalo MAR, Zanon NM, Navegantes LCC, Chaves VE, Kettelhut IDC. Glucocorticoids decrease thermogenic capacity and increase triacylglycerol synthesis by glycerokinase activation in the brown adipose tissue of rats. *Lipids.* 2022;57(6):313–25.
- Deng J, Guo Y, Yuan F, Chen S, Yin H, Jiang X, Jiao F, Wang F, Ji H, Hu G, et al. Autophagy Inhibition prevents glucocorticoid-increased adiposity via suppressing BAT whitening. *Autophagy.* 2020;16(3):451–65.
- Campbell JE, Peckett AJ, D'souza AM, Hawke TJ, Riddell MC. Adipogenic and lipolytic effects of chronic glucocorticoid exposure. 2011; 300(1):C198–209.
- Thuzar M, Law WP, Ratnasingam J, Jang C, Dimeski G, Ho KKY. Glucocorticoids suppress brown adipose tissue function in humans: A double-blind placebo-controlled study. *Diabetes Obes Metab.* 2018;20(4):840–8.
- Zeng X, Jedrychowski MP, Chen Y, Serag S, Lavery GG, Gygi SP, Spiegelman BM. Lysine-specific demethylase 1 promotes brown adipose tissue thermogenesis via repressing glucocorticoid activation. *Genes Dev.* 2016;30(16):1822–36.
- Beaupere C, Liboz A, Fève B, Blondeau B, Guillemain G. Molecular mechanisms of Glucocorticoid-Induced insulin resistance. *Int J Mol Sci.* 2021, 22(2).
- Chimin P, Farias Tda S, Torres-Leal FL, Bolsoni-Lopes A, Campaña AB, Andreotti S, Lima FB. Chronic glucocorticoid treatment enhances lipogenic activity in visceral adipocytes of male Wistar rats. *Acta Physiologica (Oxford England).* 2014;211(2):409–20.
- Lee MJ, Pramyothin P, Karastergiou K, Fried SK. Deconstructing the roles of glucocorticoids in adipose tissue biology and the development of central obesity. *Biochim Biophys Acta.* 2014;1842(3):473–81.
- von Essen G, Lindsund E, Maldonado EM, Zouhar P, Cannon B, Nedergaard J. Highly recruited brown adipose tissue does not in itself protect against obesity. *Mol Metab.* 2023;76:101782.
- Zorova LD, Popkov VA, Plotnikov EY, Silachev DN, Pevzner IB, Jankauskas SS, Babenko VA, Zorov SD, Balakireva AV, Juhászova M, et al. Mitochondrial membrane potential. *Anal Biochem.* 2018;552:50–9.
- Wan W, Hua F, Fang P, Li C, Deng F, Chen S, Ying J, Wang X. Regulation of Mitophagy by Sirtuin Family Proteins: A Vital Role in Aging and Age-Related Diseases. 2022, 14.
- Song Y, Zhou Y, Zhou X. The role of mitophagy in innate immune responses triggered by mitochondrial stress. *Cell Communication Signal.* 2020;18(1):186.
- Huang Z, Zhang Z, Moazzami Z, Heck R, Hu P, Nanda H, Ren K, Sun Z, Bartolomucci A, Gao Y, et al. Brown adipose tissue Involution associated with progressive restriction in progenitor competence. *Cell Rep.* 2022;39(2):110575.
- Cypess AM, Lehman S, Williams G, Tal I, Rodman D, Goldfine AB, Kuo FC, Palmer EL, Tseng YH, Doria A, et al. Identification and importance of brown adipose tissue in adult humans. *N Engl J Med.* 2009;360(15):1509–17.
- Wang J-C, Gray NE, Kuo T, Harris CA. Regulation of triglyceride metabolism by glucocorticoid receptor. *Cell Bioscience.* 2012;2(1):19.
- Rosina M, Ceci V, Turchi R, Chuan L, Borcherding N, Sciarretta F, Sánchez-Díaz M, Tortolici F, Karlinsey K, Chiurchiù V, et al. Ejection of damaged mitochondria and their removal by macrophages ensure efficient thermogenesis in brown adipose tissue. *Cell Metabol.* 2022;34(4):533–e548512.
- Chouchani ET, Kazak L, Spiegelman BM. Mitochondrial reactive oxygen species and adipose tissue thermogenesis: bridging physiology and mechanisms. *J Biol Chem.* 2017;292(41):16810–6.
- Wang G, Meyer JG, Cai W, Softic S, Li ME, Verdin E, Newgard C, Schilling B, Kahn CR. Regulation of UCP1 and mitochondrial metabolism in brown adipose tissue by reversible succinylation. *Mol Cell* 2019, 74(4).
- Lichtenbelt WDM, Schrauwen P. Implications of nonshivering thermogenesis for energy balance regulation in humans. 2011, 301(2):R285–96.
- Roqueta-Rivera M, Esquejo RM, Phelan PE, Sandor K, Daniel B, Foufelle F, Ding J, Li X, Khorasanizadeh S, Osborne TF. SETDB2 links glucocorticoid to lipid metabolism through Insig2a regulation. *Cell Metabol.* 2016;24(3):474–84.
- Livingstone DE, Grassick SL, Currie GL, Walker BR, Andrew R. Dysregulation of glucocorticoid metabolism in murine obesity: comparable effects of leptin resistance and deficiency. *J Endocrinol.* 2009;201(2):211–8.
- Erkens T, Vandesompele J, Van Zeven A, Peelman LJ. Correlation between Porcine *PPARGC1A* mRNA expression and its downstream target genes in backfat and longissimus dorsi muscle. *J Appl Genet.* 2009;50(4):361–9.

Publisher's note

Springer Nature remains neutral with regard to jurisdictional claims in published maps and institutional affiliations.